General Relativistic Magnetohydrodynamic Simulations of Jet Formation with a Thin Keplerian Disk

Yosuke Mizuno[1,6], Ken-Ichi Nishikawa[1,2], Shinji Koide[3], Philip Hardee[4] and Gerald J. Fishman[5]

ABSTRACT

We have performed several simulations of black hole systems (non-rotating, black hole spin parameter $a = 0.0$ and rapidly rotating, $a = 0.95$) with a geometrically thin Keplerian disk using the newly developed RAISHIN code. The simulation results show the formation of jets driven by the Lorentz force and the gas pressure gradient. The jets have mildly relativistic speed ($\gtrsim 0.4\ c$). The matter is continuously supplied from the accretion disk and the jet propagates outward until each applicable terminal simulation time (non-rotating: $t/\tau_{\rm S} = 275$ and rotating: $t/\tau_{\rm S} = 200$, $\tau_{\rm S} \equiv r_{\rm S}/c$). It appears that a rotating black hole creates an additional, faster, and more collimated matter-dominated inner outflow ($\gtrsim 0.5\ c$) formed and accelerated by the twisted magnetic field resulting from frame-dragging in the black hole ergosphere. This is the first known simulation confirming the formation of an inner magnetically-driven, matter-dominated jet by the frame-dragging effect from a black hole co-rotating with a thin Keplerian disk threaded by a vertical magnetic field. This result indicates that jet kinematic structure depends on black hole rotation and on the initial magnetic field configuration and strength.

Subject headings: accretion, accretion disks - black hole physics - magnetohydrodynamics: (MHD) - method: numerical -relativity

---

[1]National Space Science and Technology Center, 320 Sparkman Drive, VP 62, Huntsville, AL 35805, USA; Yosuke.Mizuno@msfc.nasa.gov

[2]Center for Space Plasma and Aeronomic Research, University of Alabama in Huntsville

[3]Department of Physics, Kumamoto University, Kurokami, Kumamoto, 860-8555, Japan

[4]Department of Physics and Astronomy, The University of Alabama, Tuscaloosa, AL 35487, USA

[5]NASA-Marshall Space Flight Center, National Space Science and Technology Center, 320 Sparkman Drive, VP 62, Huntsville, AL 35805, USA

[6]NASA Postdoctoral Program Fellow/ NASA Marshall Space Flight Center

1. Introduction

Both magnetic and gravitational fields play an important role in the dynamics of matter in many astrophysical systems. In a highly conducting plasma, the magnetic field can be amplified by gas contraction or shear motion. Even when the magnetic field is weak initially, the magnetic field can grow on short time scales and influence the gas dynamics of the system. The magnetic influence on gas dynamics is particulary important for a compact object such as a black hole or a neutron star. Relativistic jets have been observed or postulated in various astrophysical objects, including active galactic nuclei (AGNs) (e.g., Urry & Pavovani 1995; Ferrari 1998), microquasars in our galaxy (e.g., Mirabel & Rodiriguez 1999), and gamma-ray bursts (GRBs) (e.g., Zhang & Mészáros 2004; Piran 2005; Mészáros 2006). The most promising mechanisms for producing the relativistic jets involve magnetohydrodynamic centrifugal acceleration and/or magnetic pressure driven acceleration from an accretion disk around the compact objects (e.g., Blandford & Payne 1982; Fukue 1990), or involve the extraction of rotating energy from a rotating black hole (Penrose 1969; Blandford & Znajek 1977).

General relativistic magnetohydrodynamics (GRMHD) codes with fixed spacetimes have been developed to investigate relativistic magnetorotators (RMRs) (e.g., Koide et al. 1998; De Villiers & Hawley 2003; Gammie et al. 2003; Komissarov 2004; Antón et al. 2005; Anninos et al. 2006). These codes have been used to study the Blandford-Znajek effect near a rotating black hole (Koide 2003; Komissarov 2005; McKinney 2005), and the formation of GRB jets in collapsars (Mizuno et al. 2004a, 2004b; De Villiers et al. 2005b).

Recently, in order to investigate the properties of accretion flows onto a black hole associated with the magneto-rotational instability (MRI) (Balbus & Hawley 1991), many simulations have been performed using a thick torus-like disk (the disk thickness $H/r > 0.1$, where H is height of the disk and r is radius from a black hole) with weak poloidal magnetic fields in a torus (the plasma beta, $\beta = p_{\rm gas}/p_{\rm mag} > 100$, where $p_{\rm gas}$ is gas pressure and $p_{\rm mag}$ is magnetic pressure) (De Villiers et al. 2003, 2005a; Krolik et al. 2005; Hawley & Krolik 2006; Beckwith et al. 2006; McKinney & Gammie 2004; McKinney 2006). The initial "poloidal-loop" magnetic fields in the torus contribute to the generation of MRI, diffusion of matter and magnetic field, and jet generation. However, in their simulations the structure of magnetic fields that piled up and twisted near the black hole is different from the magnetic fields which are twisted by a thin Keplerian disk and/or the frame-dragging effect of the rotating black hole ($H/r \sim 0.06$) with a stronger initial vertical magnetic field ($\beta < 40$) (Koide, Shibata, & Kudoh 1998, 1999; Koide et al. 2000; Nishikawa et al. 2005). In the thin disk simulations MRI does not grow since the wavelength at the maximum growth rate is larger than the height of the thin disk. Koide et al. (2000) have found that jets are formed

from thin Keplerian accretion disks for both counter- and co-rotating black holes. In the co-rotating disk case, the jet had a two-layered structure: an inner gas pressure-driven jet, and an outer magnetically driven jet (Koide et al. 2000).

In this Letter we report on new simulations showing jet formation from the black hole magnetosphere co-rotating with a thin Keplerian disk threaded by a vertical magnetic field using the recently developed three-dimensional, GRMHD code RAISHIN (Mizuno et al. 2006). Our new result shows that an inner matter-dominated jet is generated by the magnetic field twisted in the ergosphere of the rotating black hole in addition to the outer jet formed by the co-rotating accretion disk seen by Koide et al. (2000). While our inner jet is similar the inner jet created by a counter-rotating disk found by Koide et al. (2000), in this case the inner jet is located closer to the rotation axis.

2. Numerical Method

In order to study the formation of relativistic jets from a geometrically thin Keplerian disk, we use a 2.5-dimensional GRMHD code with Boyer-Lindquist coordinates (r, θ, ϕ). The method is based on a 3+1 formalism of the general relativistic conservation laws of particle number and energy momentum, Maxwell equations, and Ohm's law with no electrical resistance (ideal MHD condition) in a curved spacetime (Mizuno et al. 2006).

In the RAISHIN code, a conservative, high-resolution shock-capturing scheme is employed. The numerical fluxes are calculated using the Harten, Lax, & van Lee (HLL) approximate Riemann solver scheme. The flux-interpolated, constrained transport scheme is used to maintain a divergence-free magnetic field. The RAISHIN code has proven to be accurate to second order and has passed numerical tests including highly relativistic cases, and highly magnetized cases in both special and general relativity. Code details and the results of code tests can be found in Mizuno et al. (2006). In the simulations presented here we use minmod slope limiter reconstruction, HLL approximate Riemann solver, flux-CT scheme and Noble's 2D method.

In our present simulations: a geometrically thin Keplerian disk rotates around a black hole (non-rotating, $a = 0.0$ or rapidly rotating, $a = 0.95$, here a is black hole spin parameter), where the disk density is 100 times higher than the coronal density. The thickness of the disk is $H/r \sim 0.06$ at $r = 10r_{\rm S}$. In the rotating black hole case the disk is co-rotating with the black hole. The background corona is free-falling into the black hole (Bondi flow). The initial magnetic field is assumed to be uniform and parallel to the rotational axis i.e., the Wald solution (Wald 1974). Our scale-free simulations are normalized by the speed of

light, c, and the Schwarzschild radius, $r_{\rm S}$, with timescale, $\tau_{\rm S} \equiv r_{\rm S}/c$. Values of the magnetic field strength and gas pressure depend on the normalized density, ρ_0. In these simulations the magnetic field strength, B_0, is set to $0.05\sqrt{\rho_0 c^2}$). These initial conditions are similar to Koide et al. (1999, 2000) but with a weaker initial magnetic field. Koide et al. (2000) used $B_0 = 0.3\sqrt{\rho_0 c^2}$. The simulations are performed in the region $1.1r_{\rm S} \leq r \leq 20.0r_{\rm S}$ (non-rotating black hole case) and $0.75r_{\rm S} \leq r \leq 20.0r_{\rm S}$ (rapidly rotating black hole case) and $0.03 \leq \theta \leq \pi/2$. We use 128×128 computational zones with logarithmic zone spacing in the radial direction (Koide et al. 1999). We assume axisymmetry with respect to the z-axis and mirror symmetry with respect to the equatorial plane. We employ a free boundary condition at the inner and outer boundaries in the radial direction through which waves, fluids, and magnetic fields can pass freely.

In our simulations, β is higher than 1 in the disk initially ($\beta \sim 40$ at $r = 5r_{\rm S}$). Therefore, in principle, MRI grows. However, the wavelength at the maximum growth rate is $\lambda_{\rm MRI} \sim v_{\rm Az}/\Omega$ where Ω is the angular velocity and $v_{\rm Az}$ is the z-component of the Alfvén velocity (e.g., Balbus & Hawley 1991, Gammie 2004). With our initial conditions, the wavelength at the maximum growth rate is larger than $0.6r_{\rm S}$ at $r = 5.0r_{\rm S}$ and larger than the disk height ($0.3r_{\rm S}$). Therefore the thin disk does not support the growth of MRI at this wavelength. Also, shorter wavelengths associated with MRI have slower growth rate and may not grow significantly on our simulation time scale with our grid resolution. Thus, our simulations investigate the physics of jet formation and the properties of the jets in the context of a black hole with a thin Keplerian disk threaded by vertical magnetic fields (using Wald solution) in the absence of significant MRI.

In contrast, previous GRMHD simulations with a thick torus have been used to study disk evolution via MRI and the resulting outflows (e.g., De Villiers et al. 2003; McKinney & Gammie 2004; McKinney 2006; De Villiers et al. 2005; Hawley & Krolik 2006). Here MRI creates turbulent structure in the thick disk, fluctuating accretion into the black hole, and unsteady outflows near the funnel wall, e.g., Hawley & Krolik (2006).

3. Results

Figure 1 shows snapshots of the density (panels (a) and (b)), plasma beta ($\beta = p_{\rm gas}/p_{\rm mag}$) distribution (panels (c) and (d)), and total velocity (panels (e) and (f)) for the non-rotating black hole case, $a = 0.0$ (left panels); and the rapidly rotating black hole case, $a = 0.95$ (right panels); at each simulation's terminal time (non-rotating: $t = 275\tau_{\rm S}$ and rotating: $t = 200\tau_{\rm S}$). The Keplerian disk at the marginally stable circular orbit ($r = 3r_{\rm S}$) rotates around the black hole in about $40\tau_{\rm S}$. In the non-rotating black hole case about 7 inner disk

rotations occurred during the simulation.

The numerical results show that matter in the disk loses angular momentum to the magnetic field and falls into the black hole. A centrifugal barrier decelerates the falling matter and produces a shock around $r = 2r_{\rm S}$. Matter near the shock region is accelerated by the $\mathbf{J} \times \mathbf{B}$ force and the gas pressure gradient in the z-direction (see the arrows in the panels in Figure 1). In the simulations, matter is continuously supplied from the accretion disk and the jet propagates outward through the outer boundary of the grid. In general, the results are similar to the previous work of Koide et al. (1998, 1999, 2000) and Nishikawa et al. (2005).

Contours of the toroidal magnetic field strength are shown by the white lines in Figs. 1c and 1d and indicate where the magnetic field is most twisted. In the non-rotating black hole case the magnetic field is twisted by the rotation of the Keplerian disk near the black hole region, propagates outwards along the poloidal magnetic field as an Alfvén wave and forms a jet. In the rapidly rotating black hole case the magnetic field is strongly twisted by the frame-dragging effect of the rotating black hole near the black hole region e.g., Figure 1d contours and Figure 2, propagates outwards as an Alfvén wave along the poloidal magentic field lines shown in Fig. 1b and forms an additional inner jet component closer to the black hole along the rotation axis.

The total velocity distribution of non-rotating and rapidly rotating black hole cases are shown in Figs. 1e and 1f. The jets in both cases have speeds greater than $0.4c$ (mildly relativistic) and the speeds are comparable to the Alfvén speeds. In the jets, toroidal velocity is the dominant velocity component (see Figs. 3a and 3d). In the rapidly rotating black hole case the velocity distribution indicates a two-component jet. The outer jet is similar to that of the non-rotating black hole case but the inner jet is not seen in the non-rotating black hole case. The inner jet is faster than the outer jet (over $0.5c$).

Figure 3 shows the distribution of various physical quantities on the $z/r_{\rm S} = 2$ surface at the terminal simulation time and allows us to examine the relationship between the twisted magnetic field and the jet velocity. In the non-rotating black hole case the jet is generated in the region $r \geq 2.7r_{\rm S}$ as shown in Figs. 1a and 3a. In this region, the toroidal velocity (v_ϕ) is the dominant velocity component. The magnetic field is twisted by the rotation of the Keplerian disk. As the jet propagates outward, the magnetic field is concentrated towards the rotation axis and the vertical component of the magnetic field, $B_{\rm z}$, becomes larger near the rotation axis. In the rapidly rotating black hole case, a jet is generated in the region $r \geq 0.5r_{\rm S}$. Now, two jet components can be seen in the velocity distribution. An inner jet is located at $0.7r_{\rm S} \leq r \leq 2.0r_{\rm S}$ and an outer jet is located at $r \geq 2.0r_{\rm S}$ (Fig. 3d). For both jet components, the toroidal velocity component is dominant. The toroidal velocity of the inner

jet is larger than that of the outer jet. Here the magnetic field near the black hole region is strongly twisted by the frame-dragging effect as shown in Fig. 2. Since the magnetic field is twisted and pinched toward the rotation axis, the z component of the magnetic field becomes large near the rotation axis (Fig. 3e), and the inner jet accelerates more rapidly than the outer jet.

To confirm the jet acceleration mechanism, we evaluate the vertical components of the Lorentz force, $\mathbf{F}_{\rm EM} = \rho_{\rm e}\mathbf{E} + \mathbf{J} \times \mathbf{B}$ and the gas pressure gradient, $\mathbf{F}_{\rm gp} = -\nabla p$ at the $z = 2.0 r_{\rm S}$ surface (e.g., Figs. 3c and 3f). Although this analysis is simpler than that of Hawley & Krolik (2006), it illustrates which force dominates jet formation, and has been used in previous work (e.g., Koide et al 1999, 2000, 2006; Mizuno et al. 2004a,b; Nishikawa et al. 2005).

This simple analysis clearly shows that the outer jet is accelerated mainly by the gas pressure gradient. The inner part of the outer jet may be accelerated partially by the Lorentz force but the Lorentz force in the outer part of the outer jet in the rapidly rotating black hole case is lower than the gas pressure gradient by an order of magnitude. The inner jet is accelerated by the Lorentz force. Therefore the acceleration mechanism is different in the inner and outer jets.

4. Summary and Discussion

We have performed simulations of jet formation from a geometrically thin accretion disk near both non-rotating and rotating black holes using the newly developed RAISHIN code (Mizuno et al. 2006). Simulation results show the formation of magnetically-driven jets accelerated by the Lorentz force and the gas pressure. In general, results are similar to those found in previous GRMHD simulations with a thin Keplerian disk (Koide et al. 1998, 1999, 2000; Nishikawa et al. 2005). However, in this study the rotating black hole creates a second, faster, and more collimated inner matter-dominated jet formed by the twisted magnetic field resulting from frame-dragging in the black hole ergosphere. Thus, kinematic jet structure depends on black hole rotation. While an inner jet is created by a counter-rotating thin Keplerian disk (Koide et al. 2000), the inner jet seen in our simulations is a new result not found in a previous co-rotating thin Keplerian disk case (Koide et al. 2000). This difference appears to be the result of the weaker initial magnetic field strength used in the present simulations. With stronger magnetic field (Koide et al. 2000), transport of angular momentum from the disk is more rapid, accreting matter falls more quickly, is decelerated by the centrifugal barrier near the black hole strongly, and generates a stronger shock. As a result, jets are accelerated by the gas-pressure rather than the Lorentz force of magnetic field twisted by frame-dragging. The jet seen in the co-rotating disk simulation in Koide et al.

(2000) corresponds to the outer jet seen in our present co-rotating disk simulation. Therefore this is a first simulation confirming the formation of an inner matter-dominated jet driven by the magnetic field twisted by the frame-dragging effect from a black hole co-rotating with a thin Keplerian disk threaded by a vertical magnetic field.

A two component jet structure has also been seen in GRMHD simulations of a black hole co-rotating with a thick torus (e.g., Hawley & Krolik 2006; McKinney 2006). One component is a matter-dominated outflow (funnel wall jet) with a mildly relativistic velocity ($\sim 0.3c$) along the centrifugal barrier accelerated and collimated by magnetic and gas pressure forces in the inner torus and the surrounding corona. This formation mechanism and jet are the same as the outer jet seen in our simulations. Therefore the funnel wall jet in Hawley & Krolik (2006) is the same as the outer jet in our GRMHD simulations. Their other component is a highly-relativistic Poynting flux dominated jet that is produced from the formation of a large scale radial magnetic field within the funnel. In our simulation, such a highly-relativistic Poynting flux dominated jet is not seen. This is likely caused by the difference in the initial magnetic field configuration. In Hawley & Krolik (2006) and McKinney (2006), there are initial "poloidal-loop" magnetic fields inside the torus. In the simulations, the magnetic field is twisted and expands from the torus as a magnetic tower and fills the funnel region (Hirose et al. 2004). In the late stage of the simulations a highly-relativistic Poynting flux dominated jet is formed in the low density regions in the funnel. On the other hand, our magnetic field vertically threads the disk and ergosphere initially. The vertical magnetic field near the black hole region is twisted by the frame-dragging effect (see Fig. 2) and forms the inner jet. The inner jet is much denser than the highly-relativistic Poynting flux dominated jet of Hawley & Krolik (2006) and McKinney (2006) because in the inner jet the matter is supplied from the accretion disk and the free-falling corona. While our jets are formed by the same basic mechanisms as in Hawley & Krolik (2006) and McKinney (2006), the different initial magnetic configuration has led to different jet properties and a slower matter dominated jet spine. Previous results with the co-rotating disk case of Koide et al. (2000) found that a stronger magnetic field suppressed the formation of the presently observed matter-dominated jet spine.

Y. M. is a NASA Postdoctoral Program fellow at NASA Marshall Space Flight Center. He thanks G. Richardson, D. Hartmann, C. Fendt, and M. Camenzind for useful discussions. K. N. acknowledges partial support by National Science Foundation awards ATM-0100997, INT-9981508, and AST-0506719, and the National Aeronautic and Space Administration award NNG05GK73G to the University of Alabama in Huntsville. P. H. acknowledges partial support by National Space Science and Technology Center (NSSTC/NASA) cooperative agreement NCC8-256 and NSF award AST-0506666 to the University of Alabama. The sim-

ulations have been performed on the IBM p690 at the National Center for Supercomputing Applications (NCSA) which is supported by the NSF and Altix3700 BX2 at YITP in Kyoto University.

REFERENCES

Anninos, P., Fragile, P. C., & Salmonson, J. D. 2005, ApJ, 635, 723

Antón, L., et al. 2006, ApJ, 637, 296

Balbus, S. A. & Hawley, J. F. 1991, ApJ,376, 214

Beckwith, K., Hawley, J. F., & Krolik, J. H. 2006, ApJ, submitted (astro-ph/0605295)

Blandford, R. D. & Znajek, R. L. 1977, MNRAS, 179, 433

Blandford, R. D. & Payne, D. G. 1982, MNRAS, 199, 883

De Villiers, J.-P. & Hawley, J. F. 2003, ApJ, 589, 458

De Villiers, J.-P., Hawley, J. F., & Krolik, J. H. 2003, ApJ, 599, 1238

De Villiers, J.-P., Hawley, J. F., Krolik, J. H., & Hirose, S. 2005a, ApJ, 620, 878

De Villiers, J.-P., Staff, J., & Ouyed, R. 2005b, in preparation (astro-ph/0502225)

Ferrari, A. 1998, ARA&A, 36, 539

Gammie, C. F., McKinney, J. C., & Tóth, G. 2003, ApJ, 589, 444

Gammie, C. F. 2004, ApJ, 614, 309

Fukue, J. 1990, PASJ, 42, 793

Hawley & Krolik 2006, ApJ, 614, 103

Hirose, S., Krolik, J., De Villiers, J. P., & Hawley, J. F. 2004, ApJ, 606, 1083

Koide, S., Shibata, K., & Kudoh, T. 1998, ApJ, 495, L63

——. 1999, ApJ, 522, 727

Koide, S., Meier, D. L., Shibata, K., & Kudoh, T. 2000, ApJ, 536, 668

Koide, S. 2003, Phys. Rev. D, 67, 104010

Koide, S., Kudoh, T., & Shibata, K. 2006, Phys. Rev. D, 74, 044005

Komissarov, S. S. 2004, MNRAS, 350, 1431

——. 2005, MNRAS, 359, 801

Krolik, J. H., Hawley, J. F., & Hirose, S. 2005, ApJ, 622, 1008

McKinney, J. C. 2005, ApJ, L5

——. 2006, MNRAS, 368, 1561

McKinney, J. C. & Gammie, C. F. 2004, ApJ, 977

Mészáros, P. 2006, Rep. Prog. Phys., in press (astro-ph/0605208)

Mirabel, I. F. & Rodríguez, L. F. 1999, ARA&A, 37, 409

Mizuno, Y., Yamada, S., Koide, S., & Shibata, K. 2004a, ApJ, 606, 395

——. 2004b, ApJ, 615, 389

Mizuno, Y., Nishikawa, K.-I., Koide, S., Hardee, P., & Fishman, G. J. 2006, ApJS, submitted (astro-ph/0609004)

Nishikawa, K.-I., Richardson, G., Koide, S., Shibata, K., Kudoh, T., Hardee, P., & Fishman, G. J. 2005, ApJ, 625, 60

Penrose, R. 1969, Nuovo Cimento, 1, 252

Piran, T. 2005, Reviews of Modern Physics, 76, 1143

Urry, C. M. & Padovani, P. 1995, PASP, 107, 803

Wald, R. M. 1974, Phys. Rev. D, 10, 1680

Zhang, B. & Mészáros, P. 2004, Int. J. Mod. Phys., A19, 2385

This preprint was prepared with the AAS LaTeX macros v5.0.

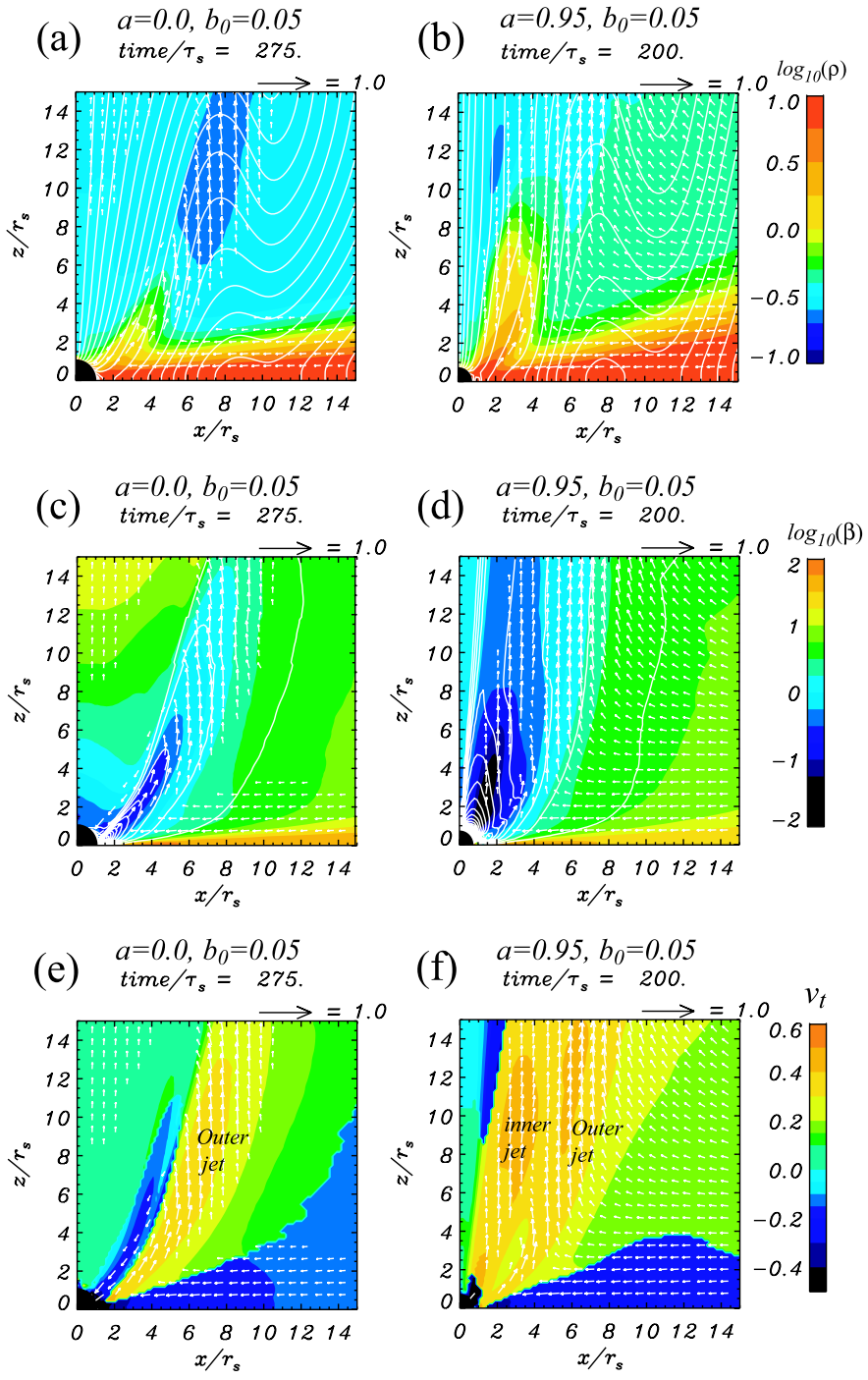

Fig. 1.— Snapshots of density and plasma beta of the non-rotating black hole case ($a = 0.0$; *a, c, e*) and the rapidly rotating black hole case ($a = 0.95$; *b, d, f*) at the applicable terminal simulation time. The color scales show the logarithm of density (upper panels), plasma beta ($\beta = p_{\rm gas}/p_{\rm mag}$; middle panels) and total velocity (lower panels). A negative velocity indicates inflow towards the black hole. The white lines indicate magnetic field lines (contour of the poloidal vector potential; upper panels) and contours of the toroidal magnetic field stength (middle panels). Arrows depict the poloidal velocities normalized to light speed, as indicated above each panel by the arrow.

Fig. 2.— Bent and twisted magnetic field lines obtained from the co-rotating black hole case at $t = 133\tau_{\rm S}$. The field lines are traced from $z = -15r_{\rm S}$ to $z = +15r_{\rm S}$ beginning at $r = 6r_{\rm S}$ (red lines) and $r = 12r_{\rm S}$ (blue lines). The black hole is indicated by the green circle.

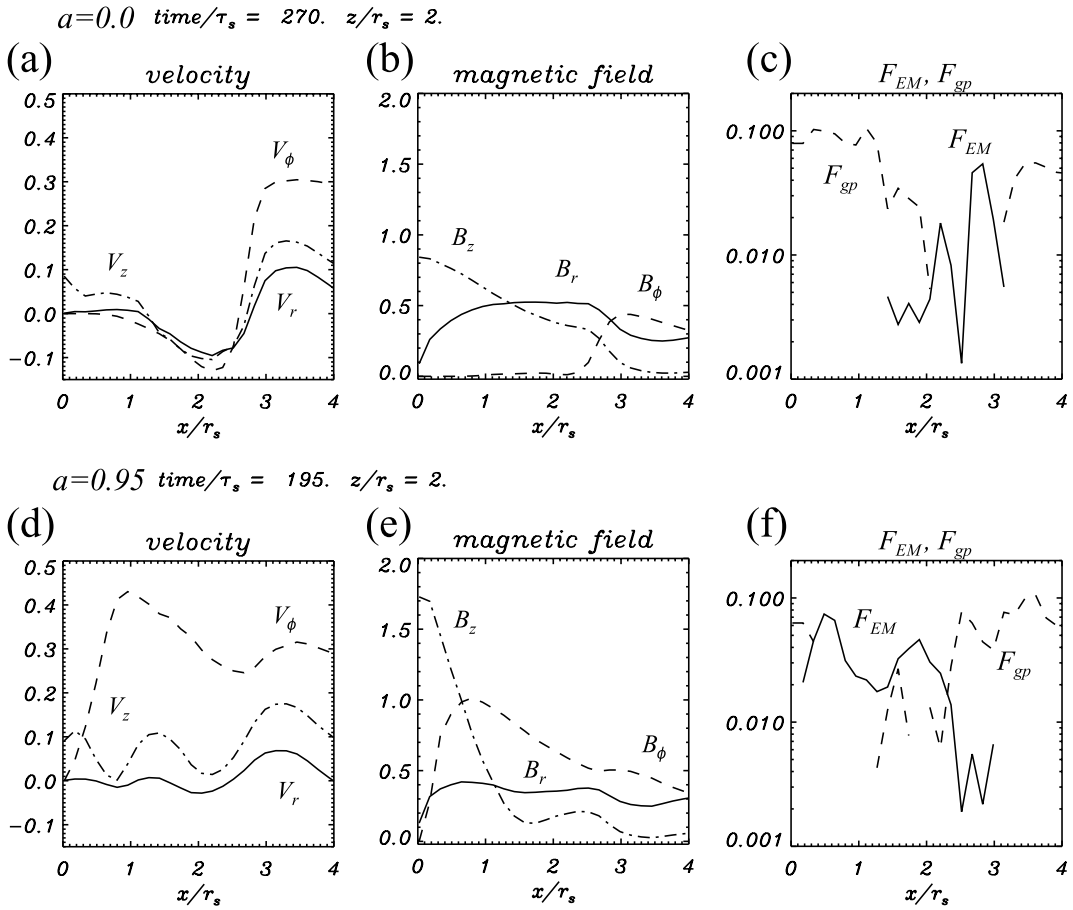

Fig. 3.— Various physical quantities on the $z/r_{\rm S} = 2$ surface at the applicable terminal simulation time. Panels *(a), (d)* show the velocity components $v_{\rm r}$ (*solid line*), v_ϕ (*dashed line*), and $v_{\rm z}$ (*dot-dashed line*). Panels *(b), (e)* show the magnetic field components $B_{\rm r}$ (*solid line*), B_ϕ (*dashed line*), and $B_{\rm z}$. (*dot-dashed line*). Panels *(c), (f)* show the z component of the Lorentz force $\mathbf{F}_{\rm EM}$ (*solid line*) and the gas pressure gradient $\mathbf{F}_{\rm gp}$ (*dashed line*).